

# Synthesis, Structure, and Kinetics and Stereochemistry of Base-Catalyzed Hydrolysis of *meso*- and *rac*-[Co<sub>2</sub>(tmpdtne)Cl<sub>2</sub>]<sup>4+</sup>, Bis(pentaamine) Complexes Devoid of Deprotonatable NH Centers

W. Gregory Jackson,\* Alistair J. Dickie, and Josephine A. McKeon

School of Physical, Environmental and Mathematical Sciences, Chemistry, University College, The University of New South Wales, Australian Defence Force Academy, Canberra, ACT, Australia 2600

Leone Spiccia and Suzanne J. Brudenell

Chemistry Department, Monash University, Clayton, Victoria, Australia 3168

David C. R. Hockless and Anthony C. Willis

Research School of Chemistry, Australian National University, Canberra, ACT, Australia 0200

Received July 6, 2004

The bis(pentadentate) ligand tmpdtne binds two Co(II) centers, and the entity is readily oxidized to the dicobalt(III) derivative [Co<sub>2</sub>(tmpdtne)Cl<sub>2</sub>]<sup>4+</sup> which has been separated into two isomeric forms. NMR studies establish these as *meso* and *rac* isomers arising from the different or same absolute configurations for the asym configuration about each Co(III) center. Each dinuclear ion base hydrolyses to the dihydroxo derivative [Co<sub>2</sub>(tmpdtne)(OH)<sub>2</sub>]<sup>4+</sup> with retained asym configurations about each metal ion and also retained *rac* or *meso* configurations. The kinetics for the stepwise loss of the two Cl<sup>-</sup> ligands is uniphaseic, and data are presented to show that the loss of the first chloride is rate determining and is followed by very rapid intramolecular and loss of the second Cl<sup>-</sup> via a hydroxo-bridged species to yield the observed dihydroxo derivative. *Meso* and *rac* forms of the latter have been crystallized. The X-ray crystal structure of the *rac*-dihydroxo complex is reported, and it establishes the configurations of all the complexes reported. The <sup>1</sup>H NMR spectra for the hydroxo ions show very high field Co–OH resonances (ca. δ –0.5 ppm) not observed previously for such ions, and this result is discussed in the context of published <sup>1</sup>H NMR data for bridged Co–OH–Co species. The base hydrolysis kinetics for the dichloro ions are first order in [OH<sup>-</sup>], and deprotonation at an α-CH<sub>2</sub> center (α to a pyridyl) is identified as the source of the catalysis, since there is no NH center available for deprotonation on the ligand. These data further support the new pseudoaminate base hydrolysis mechanism first reported in 2003. The values of *k*<sub>OH</sub> for the second-order base-catalyzed reaction are ca. 4.0 M<sup>-1</sup> s<sup>-1</sup> for both the *rac* and *meso* isomers, and these results are discussed in terms of the increased acidities of these 4+ cations compared to their 2+ ion counterparts.

## Introduction

Spiccia et al have described the synthesis<sup>1</sup> of the potentially dinucleating ligand tmpdtne derived from dtne (Figure 1) and described first by Takamoto<sup>2</sup> and later Wiegardt<sup>3</sup> and have reported on some of its metal ion chemistry.<sup>4–7</sup>

\* Author to whom correspondence should be addressed. E-mail: wgj@adfa.edu.au.

(1) Brudenell, S. J.; Spiccia, L.; Tiekink, E. R. T. *Inorg. Chem.* **1996**, *35*, 1974.

A particular interest in this ligand developed from the fact that it was devoid of NH centers, and it provided an opportunity to demonstrate that its Co(III) complexes could

- (2) Tanaka, N.; Kobayashi, Y.; Takamoto, S. *Chem. Lett.* **1977**, 107.  
 (3) Wiegardt, K.; Tolksdorf, I.; Herrman, W. *Inorg. Chem.* **1985**, *24*, 1230.  
 (4) Brudenell, S. J.; Spiccia, L.; Bond, A. M.; Mahon, P. C.; Hockless, D. C. R. *J. Chem. Soc., Dalton Trans.* **1998**, 3919.  
 (5) Spiccia, L.; Fallon, G. D.; Grannas, M. J.; Nichols, P. J.; Tiekink, E. R. T. *Inorg. Chim. Acta* **1998**, *279*, 192.

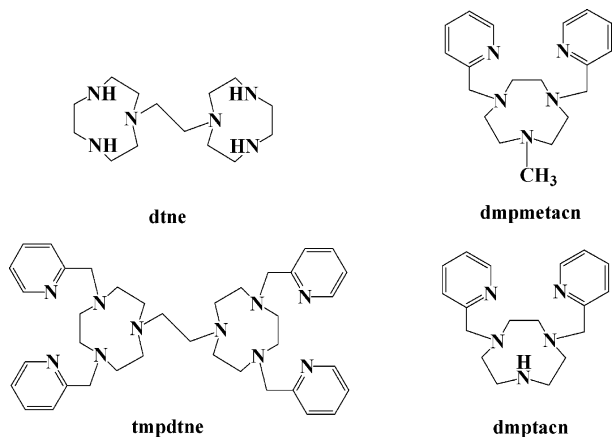
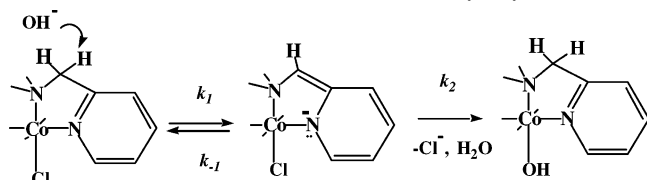


**Figure 1.** Bis(pentadentate) and other pentadentate ligands.

**Scheme 1.** Pseudoaminate Mechanism of Base Hydrolysis



hydrolyze *without* base catalysis. For cobalt(III) amine complexes, this has been an outstanding problem since amine complexes devoid of acidic NH centers have previously proved difficult if not impossible to synthesize.<sup>8</sup>

Our first attempt to examine this aspect of the normally accepted base-catalyzed hydrolysis mechanism ( $S_N1CB$ ) entailed the ligands dmptacn and dmpmetacn (Figure 1).<sup>9,10</sup> The complex of each can exist in asym and sym forms (Figure 2), but only the asym isomers have been isolated thus far.

We discovered that the complex of the dmpmetacn ligand base hydrolyzed by a pathway first order in  $[OH^-]$ .<sup>9</sup> Moreover, the reaction was faster than that for its unsubstituted analogue, dmptacn, which bears a single NH center. These studies uncovered a new mechanism for base-catalyzed substitution, whereby deprotonation at a methylene center  $\alpha$  to a pyridyl can generate an activating aminate ion, Scheme 1.

This work provides further evidence for this unique mechanism and also examines the stereochemistry of the substitution process. In addition, it was of interest to see if the two pentaaminechlorocobalt(III) centers of the dinuclear complex of tmpdtne (Figure 3) behaved independently or otherwise in base-catalyzed hydrolysis; the expectation for remote and noninteracting cobalt centers was for sequential hydrolysis with the two rates related statistically, 2:1.

## Experimental Section

All chemicals were AnalaR or an equivalent grade. Carbon-13 and proton NMR spectra and were recorded on Varian XL-300 and Unity Plus 400 MHz instruments at 20 °C. Solvents used were  $D_2O$  with dioxane as the internal reference ( $^{13}C$ ,  $\delta$  69.27 relative to DSS) and  $Me_2SO-d_6$  with the central peak of the  $CD_3$  septet as the reference ( $^{13}C$ ,  $\delta$  39.37 relative to  $SiMe_4$ ). Visible/UV absorption spectra (300–600 nm) and absorbance–time traces were recorded on a HP8453 diode array spectrophotometer thermostated to  $25.00 \pm 0.05$  °C with use of a Lauda RM6 circulating water bath. Infrared spectra were obtained for KBr disks on a Biorad FTIR instrument. Cation-exchange media used were Dowex 50Wx2 ( $H^+$  form, 200–400 mesh; Biorad) and SP-Sephadex C25 ( $Na^+$  form; Pharmacia). Electrospray ionization mass spectra were recorded on either a Micromass Platform QMS with electrospray source or a Bruker BioApex 47e FTMS with a 4–7 T superconducting magnet and Analytica electrospray source. Carbon dioxide free Milli-Q water was used for all physical measurements.

**Syntheses.** The free dtne base was made from the hydrobromide  $dtne \cdot 6HBr \cdot 2H_2O$ .<sup>3</sup> Subsequent reaction with 4 equiv of picolyl chloride provided tmpdtne as described.<sup>1</sup> The dichlorocobalt(III) complex of the crude ligand was prepared by any of the three methods described for the mononuclear chloro complexes of dmpmetacn and dmptacn.<sup>9,10</sup> The best is the reaction of free tmpdtne base with 2 equiv of *trans*- $[Co(py)_4Cl_2]Cl \cdot 6H_2O$ <sup>11</sup> in warm MeOH. The deep pink product was purified by ion exchange chromatography on a short Dowex column by elution with 4–5 M HCl. Crystallization from water using a fifth volume of  $HClO_4$  (70%) gave a quantitative precipitation of the very insoluble perchlorate salt. It was recrystallized from a concentrated solution in  $Me_2SO$  by careful dilution with 1 M aqueous  $NaClO_4$ . It was collected, washed with ethanol and ether, and air-dried. Anal. Calcd for  $Co_2(C_{38}H_{52}N_{10})Cl_2(ClO_4)_4 \cdot 2H_2O$ : C, 35.9; H, 4.4; N, 11.0. Found: C, 35.7; H, 4.4; N, 10.8. Vis/UV ( $CH_3CN$ ):  $\epsilon_{370}$   $572 M^{-1} cm^{-1}$  and  $\epsilon_{508}$   $504 M^{-1} cm^{-1}$ ; these values are very similar to those for their mononuclear analogues, save for the factor of 2 in the  $\epsilon$  values. They were used to determine the stoichiometry of other salts from their vis/UV spectra.

**Caution!** Perchlorate salts of metal complexes containing organics are potentially explosive. They should be handled only in small quantities and never be heated in the solid state nor in solutions of neat organic solvents especially in the presence of concentrated  $HClO_4$ .

The quite soluble chloride salt was conveniently obtained from the purified perchlorate by adding some HCl (10 M) to a slurry of the salt in acetone/water (1:1) and then carefully diluting with excess acetone.

Chromatography on a long (50 cm) Dowex column, again using HCl (4–5 M) as eluant, cleanly separated the material into two pink bands in comparable amounts. The *rac-asym-asym*- $[Co_2(tmpdtne)Cl_2]^{4+}$  isomer elutes in front of the meso form; each was crystallized as chloride and perchlorate salts as described for the mixture. Tetrachlorozincate salts were also obtained, using “ $H_2-ZnCl_4$ ” (2 M  $ZnCl_2$  in 5 M HCl) as the precipitant.

**Equilibration of the meso- and rac-asym-asym- $[Co_2(tmpdtne)Cl_2]Cl_4$  Complexes.** A sample (0.1 g) of either the meso or rac species was dissolved in water (10 mL), and excess zinc dust (0.1 g) was added to the pink solution. On being stirred, the solution quickly decolorized. It was filtered and allowed to reoxidize in air; HCl was added (to the 5 M level), and the solution was heated (90 °C, 1 h). Chromatography on Dowex as above yielded two separate

- (6) Brudenell, S. J.; Spiccia, L.; Bond, A. M.; Comba, P.; Hockless, D. C. R. *Inorg. Chem.* **1998**, *37*, 3705.  
 (7) Brudenell, S. J.; Spiccia, L.; Bond, A. M.; Fallon, G. D.; Hockless, D. C. R.; Lazarev, G.; Mahon, P. J.; Tiekink, E. R. T. *Inorg. Chem.* **2000**, *39*, 881.  
 (8) Jackson, W. G. *Inorg. React. Mech.* **2002**, *4*, 1.  
 (9) Dickie, A. J.; Hockless, D. C. R.; Willis, A. C.; McKeon, J. A.; Jackson, W. G. *Inorg. Chem.* **2003**, *42*, 3822.  
 (10) Jackson, W. G.; Bhula, R.; McKeon, J. A.; Brudenell, S. J.; Spiccia, L.; Hockless, D. C. R.; Willis, A. C. *Inorg. Chem.* **2004**, *43*, 6549.

- (11) Springborg, J.; Schaffer, C. E. *Acta Chem. Scand.* **1973**, *27*, 3312.

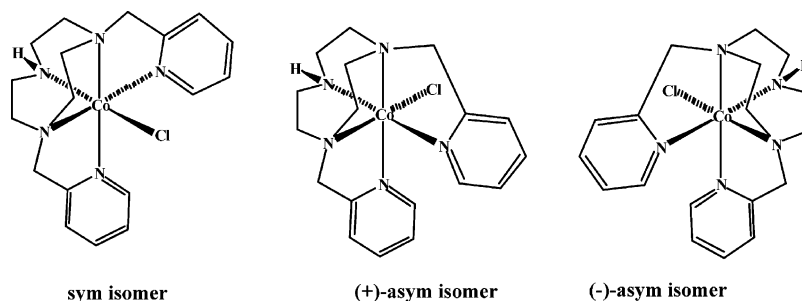


Figure 2. Two geometric isomers for [Co(dmptacn)X]<sup>n+</sup>.

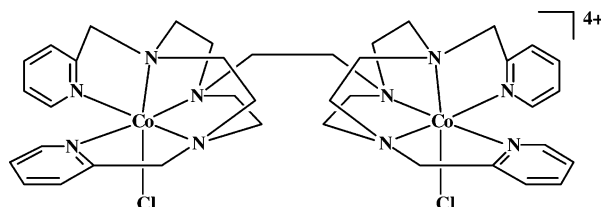


Figure 3. Dinuclear chlorocobalt(III) complex of tmpdtne.

pink bands in comparable amounts which were isolated by crystallization as their perchlorate salts and shown to be the rac (band 1) and meso (band 2) complexes, respectively.

**[Co<sub>2</sub>(tmpdtne)(OH)<sub>2</sub>](ClO<sub>4</sub>)<sub>4</sub>·5H<sub>2</sub>O.** To a concentrated solution of the chloro derivative (meso or rac; chloride salt) in water (1.0 g/15 mL) was added 2 M NaOH (4 mL). Within 1 min hydrolysis was complete, and a fifth volume of NaClO<sub>4</sub> (5 M) was added and the mixture set on ice. Deep red-pink crystals deposited in good yield (90%). The complexes were recrystallized from 0.01 M NaOH again using NaClO<sub>4</sub> as precipitant. These were filtered out, washed with *i*-PrOH and ether, and air-dried. Anal. Calcd for Co<sub>2</sub>C<sub>38</sub>H<sub>54</sub>N<sub>10</sub>(OH)<sub>2</sub>(ClO<sub>4</sub>)<sub>4</sub>·5H<sub>2</sub>O: C, 35.4; H, 5.0; N, 10.9; Cl, 11.0. Found: C, 35.2; H, 4.5; N, 10.6; Cl, 10.9. The rac isomer proved to be a trihydrate (X-ray structure).

**Steric Course of Base Hydrolysis.** A sample (ca. 80 mg) of meso- or rac-asym-asym-[Co<sub>2</sub>(tmpdtne)Cl<sub>2</sub>]<sup>4+</sup> (Cl<sup>-</sup> salt) was dissolved in D<sub>2</sub>O (0.8 mL) containing dioxane as an internal reference, and the <sup>1</sup>H and <sup>13</sup>C NMR spectra were recorded. Two drops of NaOD (10 M) were then added, and the NMR spectra were recorded for the hydroxo ion that was formed within seconds (established in control experiments). The product solution was acidified by addition of several drops of DCl (10 M) until the solution just became orange; protonation of the ligand does not involve rearrangement about the metal ion. The <sup>1</sup>H and <sup>13</sup>C NMR spectra were again recorded.

**Buffer Solutions.** Buffers employed ethanolamine (0.40 M), partly neutralized (0.1–0.9 equiv) with HCl, with the ionic strength adjusted to 2.00 M with NaCl. They were diluted 1:1 for use. The p[H] determinations were performed as previously described.<sup>9</sup>

**Base Hydrolysis Kinetics.** The kinetics for the dichloro species were measured in a series of buffers at 25.00 ± 0.05 °C. NaCl rather than NaClO<sub>4</sub> was used as the supporting electrolyte because of solubility limitations. All rates were measured as absorbance versus time traces in triplicate, using the in situ method (1 cm cell).<sup>9</sup> Either the chloride or perchlorate salts (ca. 0.01 g) were used for all kinetic runs. These were carried out by thermally equilibrating equal volumes (1.00 mL) of each of a solution of the complex and the double-concentration buffer (2 M) in a bifurcated 1 cm cell and mixing rapidly to initiate reaction. Kinetic data were analyzed by weighted (1/σ<sup>2</sup>) nonlinear regression using Kaleidagraph running on a Macintosh or by importing the HP mkd files into Specfit and carrying out Global Spectral Analysis (SVD data reduction) to a first-order rate law.<sup>9</sup>

Table 1. Crystal Data for rac-asym-asym-[Co<sub>2</sub>(tmpdtne)(OH)<sub>2</sub>](ClO<sub>4</sub>)<sub>4</sub>·3H<sub>2</sub>O

formula	C <sub>38</sub> H <sub>62</sub> Cl <sub>4</sub> Co <sub>2</sub> N <sub>10</sub> O <sub>21</sub>
<i>M</i>	1254.64
cryst system	monoclinic
space group	<i>P</i> 2 <sub>1</sub> / <i>a</i>
<i>a</i> /Å	13.331(3)
<i>b</i> /Å	23.353(5)
<i>c</i> /Å	16.478(4)
β/deg	94.98(2)
<i>V</i> /Å <sup>3</sup>	5111(2)
<i>Z</i>	4
<i>T</i> /K	296.2
λ(Cu Kα)/Å	1.5418
<i>D</i> <sub>c</sub> /g cm <sup>-3</sup>	1.631
μ/cm <sup>-1</sup>	77.8
no. of obsd/unique data	8189/7586 (1630, <i>I</i> > 3σ( <i>I</i> ))
no. of refined params	331
<i>R</i>	0.0901
<i>R</i> <sub>w</sub>	0.0764

**Crystallography.** Orange crystals of rac-asym-asym-[Co<sub>2</sub>(tmpdtne)(OH)<sub>2</sub>](ClO<sub>4</sub>)<sub>4</sub>·3H<sub>2</sub>O suitable for X-ray crystallographic analysis were grown by slow evaporation of an aqueous solution. An orange prismatic crystal having the approximate dimensions of 0.28 × 0.12 × 0.08 mm was mounted on a glass fiber. All measurements were made at 23 °C on a Rigaku AFC6R diffractometer with graphite-monochromated Cu Kα radiation. Crystal data are given in Table 1.

The structure was solved by direct methods.<sup>12</sup> Owing to the lack of sufficiently intense reflection data, only Co and Cl atoms were refined with anisotropic displacement parameters and other non-H atoms were refined isotropically. H atoms attached to other atoms were included at geometrically determined positions and were not refined. All calculations were performed using the teXsan crystallographic software package of Molecular Structure Corp.<sup>13</sup>

## Results and Discussion

**Synthesis and Characterization.** The elution characteristics, microanalyses, and vis/UV spectra for the new dinuclear complexes were consistent with the formulation [Co<sub>2</sub>(tmpdtne)Cl<sub>2</sub>]<sub>*X*</sub> (*X*<sub>*n*</sub> = Cl<sub>4</sub>, (ClO<sub>4</sub>)<sub>4</sub>, or (ZnCl<sub>4</sub>)<sub>2</sub>). The microprobe and electro spray mass spectrum indicated a Co:Cl ratio of 1:3 for the perchlorate salt, while the IR spectrum showed peaks at 1090 and 625 cm<sup>-1</sup> attributable to ClO<sub>4</sub><sup>-</sup>, absorptions in the range 1400–1620 cm<sup>-1</sup> assignable to C=C and C=N of pyridine, and a characteristic strong absorption at 3420 cm<sup>-1</sup> due to lattice water. The <sup>1</sup>H (Figure 4) and <sup>13</sup>C (Figure 1S, Supporting Information) NMR spectra

- (12) Altomare, A.; Cascarano, G.; Giacovazzo, C.; Guagliardi, A.; Burla, M. C.; Polidori, G.; Camalli, M. *J. Appl. Crystallogr.* **1994**, *27*, 435.  
 (13) *teXsan. Single-Crystal Structure Analysis Software*, version 1.7; Molecular Structure Corp.: 3200 Research Forest Drive, The Woodlands, TX 77381, 1992–1997.

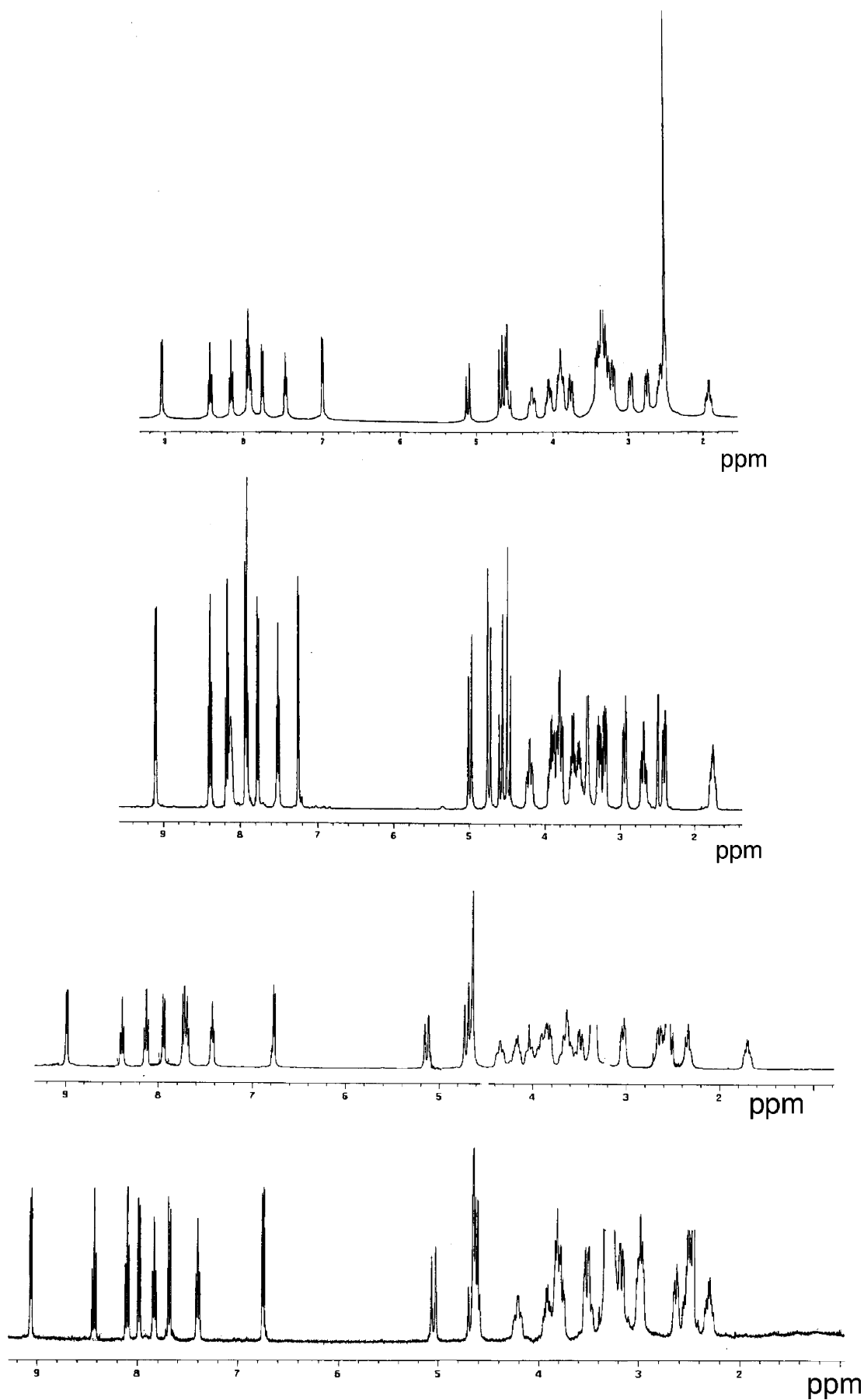


**Figure 4.**  $^1\text{H}$  NMR spectra (top to bottom) for  $\text{asym-}[\text{Co}(\text{dmpmetacn})\text{Cl}]^{2+}$ ,  $\text{asym-}[\text{Co}(\text{dmptacn})\text{Cl}]^{2+}$ , and  $\text{rac-}$  and  $\text{meso-asym-asym-}[\text{Co}_2(\text{tmpdtne})\text{Cl}_2]^{4+}$  in  $\text{Me}_2\text{SO-}d_6$ .

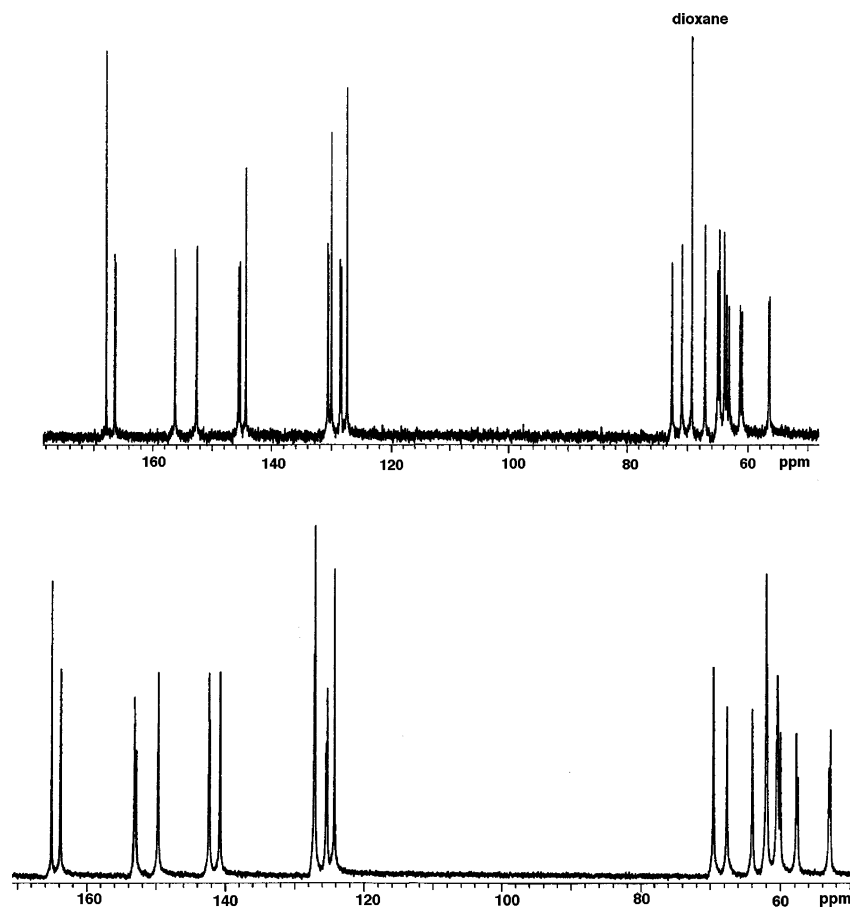


**Figure 5.** <sup>13</sup>C NMR spectra for *asym-asym*-[Co<sub>2</sub>(tmpdtne)Cl<sub>2</sub>]<sup>4+</sup> complexes in D<sub>2</sub>O (top) and Me<sub>2</sub>SO-*d*<sub>6</sub> (bottom). The doubling in some peaks is due to the presence of two isomers of very similar configurations.

for each isomer were almost identical. The highest field peak in the <sup>13</sup>C NMR spectra represents the bridging ethylene carbons, and the chemical shifts for other signals are clearly indicative of dinuclear cations that closely resemble those for *asym*-[Co(dmptacn)Cl]<sup>2+</sup> and *asym*-[Co(dmpmetacn)Cl]<sup>2+</sup> which are also shown. Moreover, the two *asym* “halves” of each dinuclear cation are symmetry related. Figure 5 shows the <sup>13</sup>C spectra for the mixture prior to separation where partial doubling of the peaks first alerted us to the presence of two isomers.

There are four possible geometric isomers for these dinuclear species: *sym-sym*, *asym-sym*, and *asym-asym*, the last of which has *meso* and *racemic* forms (Figure 6). The second and last isomers are, in principle, optically resolvable. The observation of 19 lines (19 × 2C) in the <sup>13</sup>C NMR spectra eliminates the *sym-sym* form which should show only 10 lines (9 × 4C + 1 × 2C). Further, the *sym-asym* form is eliminated on the basis that this has no symmetry and should show 38 lines. Two halves of the molecule are reasonably remote such that there would be 18 lines for the *asym* “half” while the *sym* portion should show 18 lines also but in closely spaced doublets due to the chiral *asym* component rendering the 9 pairs of *sym* carbons diastereotopic. By the same argument, the spectra for the two *asym-asym* isomers (*rac* and *meso*) should be very similar, as indeed they are. The two halves are symmetry related (*C*<sub>2</sub> or *σ*), and the spectra show just 19 lines each.

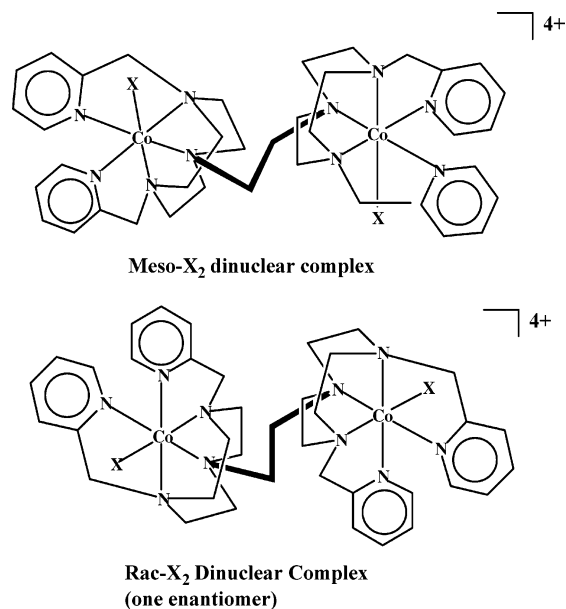


**Figure 6.** Two topologies possible for *asym-asym*-[Co<sub>2</sub>(tmpdtne)X<sub>2</sub>]<sup>n+</sup>.

Finally, we note that Zn reduction of either dichloro isomer yields the labile Co(II) species which after removal of the zinc undergoes ready aerial reoxidation to yield an ca. 1:1 mixture of the *rac* and *meso* isomers, converted to the dichloro species using hot HCl. This proved to be a useful way of synthesizing one isomer from the other.

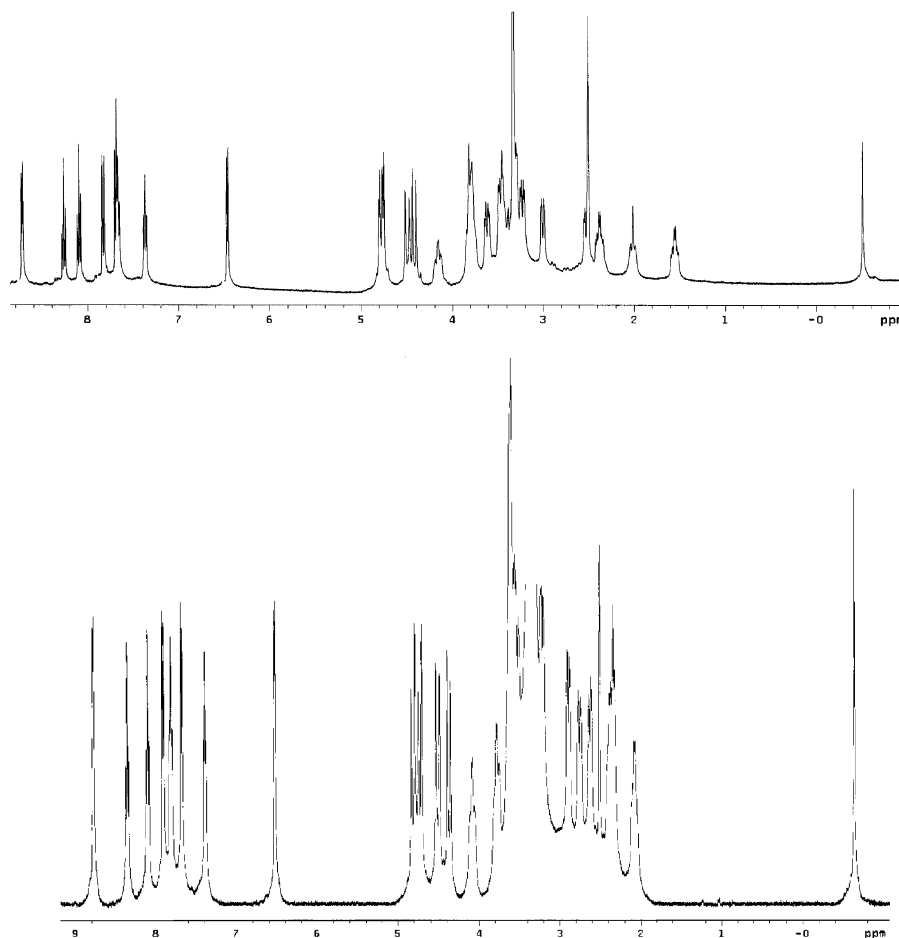


**Figure 7.**  $^1\text{H}$  NMR spectra for the *rac*- (top) and *meso*- (bottom) *asym-asym*- $[\text{Co}_2(\text{tmpdne})(\text{OH})_2](\text{ClO}_4)_4 \cdot x\text{H}_2\text{O}$  complexes in  $\text{Me}_2\text{SO}-d_6$ , illustrating the same *asym* configuration about cobalt and the very high field Co–OH signals.

**Stereochemistry of Substitution.** Both the *rac* and *meso* complexes hydrolyzed through to the dihydroxo ions with complete retention. The intermediate hydroxochloro ions were not observed. The dihydroxo ions in hot HCl revert to the dichloro ions with complete retention. These results are consistent with those determined for the mononuclear analogues *asym*- $[\text{Co}(\text{dmpmetacn})\text{Cl}]^{2+}$  and *asym*- $[\text{Co}(\text{dmp-tacn})\text{Cl}]^{2+}$  where retention was established by using a regiospecifically D-labeled reactant for the former species<sup>9</sup> and an optically resolved sample of the latter.<sup>10</sup>

The dihydroxo complexes derived from the respective dichloro complexes were isolated, and the X-ray structure of one of these species (*vide infra*) established that the faster eluting dichloro ion was the *rac* complex. The  $^1\text{H}$  (Figure 7) and  $^{13}\text{C}$  NMR spectra (Figure 2S, Supporting Information) are analogous to those of the dichloro ions, save for the very high field proton signals at ca.  $-0.5$  ppm which are assigned to the Co–OH residue. Initially these were believed to be due to bridging OH, but they integrated for 2H and for a bis(pentaamine) species only a single OH bridge is possible. Very high field signals ( $<0$  ppm) are characteristic of bridging OH,<sup>14</sup> and it now seems terminal Co–OH are also at high field (but not as high field as bridging OH). There

are few data for such complexes, but we have confirmed that the OH signal for  $[\text{Co}(\text{NH}_3)_5\text{OH}](\text{ClO}_4)_2$  measured in very dry  $\text{Me}_2\text{SO}-d_6$ <sup>15</sup> is also to higher field of  $\text{SiMe}_4$  (cf. the  $\delta$  5.6 ppm signal for the aqua protons in  $[\text{Co}(\text{NH}_3)_5\text{OH}_2](\text{ClO}_4)_3$ <sup>16</sup>).

**Kinetics.** The observation of uniphase kinetics under all conditions for both the *meso* and *rac* dinuclear complexes was at first surprising. Consecutive reactions were anticipated, dichloro to monochloro followed by monochloro to dihydroxo complex. Moreover, the relative rates for the two steps were expected to be ca. 2:1, reflecting the statistics for the two phases—the reactant of charge 4+ bearing two  $\text{Cl}^-$  and the intermediate species, also of charge 4+, having just the one  $\text{Cl}^-$ . It has been pointed out that, for reactions involving two phases, relationships may exist between rate constants and extinction coefficients such that there can be “accidental” single exponential behavior; one can be measuring either  $k_1$  or  $k_2$  depending upon the particular relationship.<sup>17</sup> Furthermore, where the two rate constants are within a factor of 2, consecutive reactions can be intrinsically

(14) Angus, P. M.; Fairlie, D. P.; Gunasingam, R.; Zhu, T.; Jackson, W. G. *Inorg. Chim. Acta* **1993**, *209*, 123.

(15) The OH protons exchange in  $\text{D}_2\text{O}$  but are clear sharp singlets in the aprotic solvent  $\text{Me}_2\text{SO}$  provided it is not “wet”; terminal Co–OH exchange readily in “wet” solvent, and an average OH/OH<sub>2</sub> signal is observed, whereas separate OH and OH<sub>2</sub> signals are nonetheless observed for bridging OH species.

(16) Buckingham, D. A.; Cresswell, P. J.; Jackson, W. G.; Sargeson, A. M. *Inorg. Chem.* **1981**, *20*, 1647.

difficult to resolve into two exponentials,<sup>18,19</sup> and this was anticipated to be true of the present systems. In such circumstances a fit to a single exponential is usually quite good, and the rate constant extracted can be more or less than  $k_1$  or  $k_2$  depending upon the extinction coefficient relationships among reactant, intermediate, and product.

One resolution of the problem is to detect and measure the intermediate. Thus the base hydrolysis reaction was quenched at a time that maximized the concentration of the supposed intermediate species, for a  $k_1:k_2$  rate ratio sequence of 2:1, and the product distribution was determined by ion exchange chromatography. Only recovered reactant (4+) and the disubstituted product [Co<sub>2</sub>(tmpdtne)(OH<sub>2</sub>)<sub>2</sub>]<sup>6+</sup> were observed; there was no detectable intermediate [Co<sub>2</sub>(tmpdtne)(OH<sub>2</sub>)Cl]<sup>5+</sup> species. This result is consistent with a slow-fast sequence with the second step more than 20-fold faster than the first, an anomalous result discussed in the next section. The measured rate constant is therefore  $k_1$ .

The rates of base hydrolysis for the *meso* and *rac* forms as a function of [OH<sup>-</sup>] are shown in Figure 8 (Table 1S, Supporting Information).

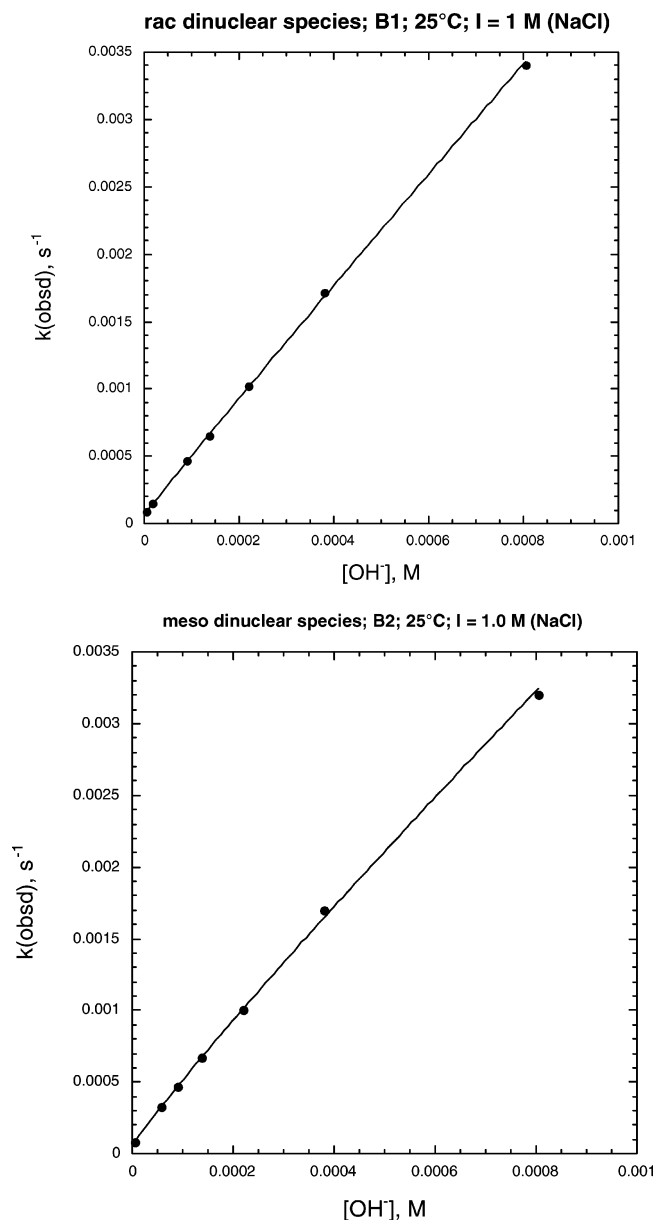
The curve fits were by weighted nonlinear least squares.<sup>10</sup> The dependences are essentially linear, with finite but small intercepts which correspond to the acid hydrolysis rates ((6.0 ± 0.5) × 10<sup>-5</sup> s<sup>-1</sup> for each, comparable to the corresponding rates for the mononuclear ions derived from dmptacn and dmpmetacn<sup>9,10</sup>). The slopes give  $k_{OH}$ , and these values are also essentially identical for the two isomers (*rac*,  $k_{OH} = 4.7 ± 0.05$  and  $4.2 ± 0.05$  M<sup>-1</sup> s<sup>-1</sup>; *meso*,  $k_{OH} = 5.5 ± 0.3$  and  $4.0 ± 0.1$  M<sup>-1</sup> s<sup>-1</sup>; 25 °C,  $I = 1.0$  M, NaCl). The two values for each complex correspond to different medium effects<sup>20</sup> at low and higher pH, as discussed elsewhere;<sup>10</sup> the curve for the *meso* isomer is slightly more pronounced. The close similarity of the *rac* and *meso* rates is not surprising since the two Co(III) centers are remote (-CH<sub>2</sub>-CH<sub>2</sub>- connectivity). However, the fact that they *are* connected is not without several effects. First, the two dinuclear cations are formally 4+ ions, and their elution behavior from Dowex cation-exchange resin reflects the connection of two 2+ cations. The second effect, again attributable to the 4+ charge, is the expected increased acidity of a pyridine α-CH<sub>2</sub>. If the base hydrolysis occurs by rate-limiting deprotonation, then the measured rate of base hydrolysis is the rate of proton abstraction from a methylene center, which should correlate with charge (increased charge, increased acidity). Moreover,

(17) Jackson, W. G.; Harrowfield, J. M.; Vowles, P. D. *Int. J. Chem. Kinet.* **1977**, *9*, 535.

(18) Jackson, W. G.; Sargeson, A. M. *Inorg. Chem.* **1978**, *17*, 1348.

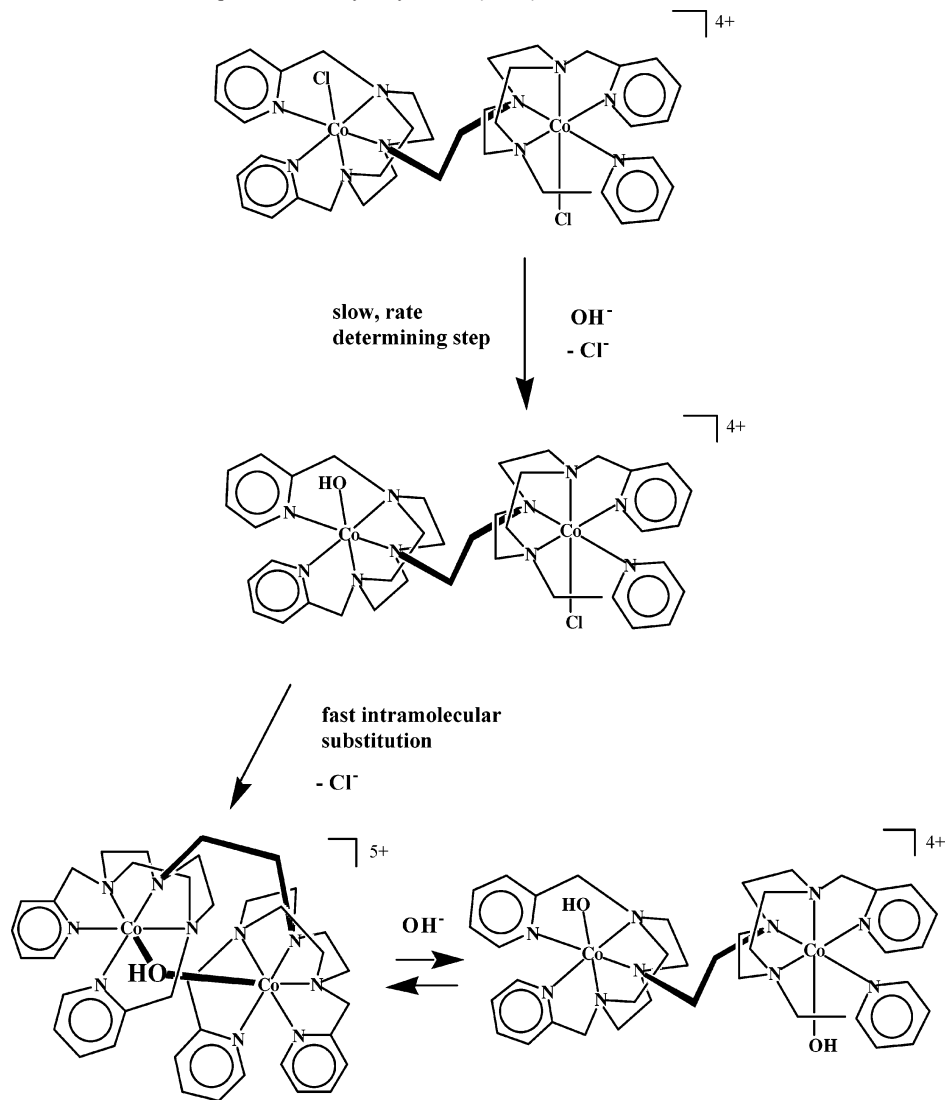
(19) Jackson, W. G.; Rahman, A. F. M. M.; Wong, M. A. *Inorg. Chim. Acta* **2004**, *357*, 665.

(20) The ethanolamine buffers used have a total base concentration of 0.2 M, and the ratio of acid to conjugate base varies between 9:1 and 1:9 for the pH range investigated. The substitution of the conjugate acid by Na<sup>+</sup>, at constant ionic strength, as the pH is raised leads to a slight medium effect. If  $k_{OH1}$  is the second-order rate constant at low pH and  $k_{OH2}$  the corresponding constant at the top [OH<sup>-</sup>] examined (8.04 × 10<sup>-4</sup> M), the observed rate constant  $k(\text{obsd}) = k_0 + f k_{OH1}[\text{OH}^-] + (1 - f)k_{OH2}[\text{OH}^-]$ , where  $k_0$  is the hydroxide-independent "acid" hydrolysis rate constant and  $f$  is that fraction of the buffer comprising the 9:1 (lowest pH) buffer component. For the buffers listed in Table 1S, these fractions are, from bottom to top, 1, 0.743 (*rac*), 0.512 (*meso*), 0.425, 0.342, 0.252, 0.145, and 0.



**Figure 8.** Rates of base hydrolysis for the *rac*- (top) and *meso*- (bottom) *asym-asym*-[Co<sub>2</sub>(tpdtne)Cl<sub>2</sub>]<sup>4+</sup> ions in ethanolamine buffers at 25 °C and  $I = 1.0$  M (NaCl).

if the complex base hydrolyses by the normal S<sub>N</sub>1CB mechanism, i.e., a fast acid–base preequilibrium followed by rate-determining loss of the leaving group, then the observed base hydrolysis rate constant  $k_{OH} = Kk$ , where  $K$  is the acidity constant. So again, the rate should correlate with the acidity. The rates of base hydrolysis of the related pyridylmethylene “armed” ligands (Figure 1) are  $k_{OH} = 0.040$  M<sup>-1</sup> s<sup>-1</sup> for *asym*-[Co(dmptacn)Cl]<sup>2+</sup> and  $k_{OH} = 0.70$  M<sup>-1</sup> s<sup>-1</sup> for *asym*-[Co(dmpmetacn)Cl]<sup>2+</sup> under the same conditions.<sup>9,10</sup> The closest to the tmpdtne complexes is the dmpmetacn complex which differs in having a CH<sub>3</sub> rather than -CH<sub>2</sub>-CH<sub>2</sub>- substituent on one of the tacn nitrogens. The 4+ *meso*- and *rac*-tmpdtne complexes are only about 3-fold more reactive, after correction for the statistical advantage (×2) that the dinuclears ions have, and this may be reasonably attributed to a slightly increased acidity.

**Scheme 2.** Proposed Mechanism for the Sequential Base Hydrolysis of *asym-asym*-[Co<sub>2</sub>(tmpdtne)Cl<sub>2</sub>]<sup>4+</sup>

**Intramolecular Substitution.** The fact that the second step proved to be much faster than the first suggested another consequence of the connected reaction centers; some special mechanism is operative for the intermediate [Co<sub>2</sub>(tmpdtne)(OH)Cl]<sup>4+</sup> complex. We excluded “double substitution”, i.e., loss of both Cl<sup>-</sup> in a single step; although a known reaction,<sup>21</sup> it requires special conditions (two leaving groups on the same metal center, as a minimum) that are absent here.

For simpler amine systems, there are a number of di- and trinuclear species known where the bridge facilitates extraordinarily rapid intramolecular substitution, either at one of the metal centers or at an activated bound ligand.<sup>22,23</sup> We propose a similar mechanism here (Scheme 2), where bound OH<sup>-</sup> attacks the other center. Note that this reaction needs no base except to maintain Co–OH rather than Co–OH<sub>2</sub> in basic solution.

The obvious reactivity of the dinuclear hydroxochloro ion and its bridging hydroxo product precluded their isolation or even the observation of their transient existence. NMR studies show that the explicit equilibrium (Scheme 2) lies to the right under the basic conditions used but in principle can be reversed by reducing the [OH<sup>-</sup>]. Thus far we have been unsuccessful in isolating a bridging hydroxo species via this route due to limited material, but molecular mechanics calculations and even Dreiding models show that this species should exist despite the perceived steric congestion problems, in both the meso and rac configurations (Figure 3S, Supporting Information). Further, given that only the first reaction is base catalyzed, it occurred to us that by raising the [OH<sup>-</sup>] the first but not the second step becomes faster, increasing the maximum concentration of accumulated intermediate species. However, despite efforts, we have been unable to observe any intermediate monochloro dinuclear ion even by operating at high [OH<sup>-</sup>] and acid (NH<sub>4</sub><sup>+</sup>) quenching at relatively short reaction times.

**Mechanism.** The first step is clearly base catalyzed, and since there are no NH centers, the base catalysis is assumed

(21) Jackson, W. G. In *The Stereochemistry of Organometallic and Inorganic Compounds*; Bernal, I., Ed.; Elsevier: New York, 1986; Vol. 1, p 255.

(22) Alcock, N. W.; Creaser, I.; Curtis, N. J.; Roecker, L.; Sargeson, A. M.; Willis, A. C. *Aust. J. Chem.* **1990**, *43*, 643.

(23) Roecker, L.; Sargeson, A. M.; Willis, A. C. *J. Chem. Soc., Chem. Commun.* **1988**, 119.



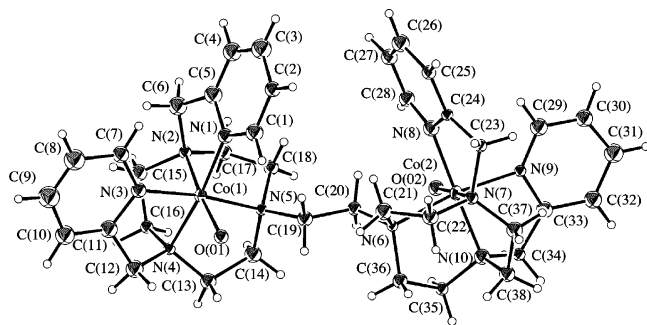


**Figure 9.** ORTEP diagram for the molecular cation *meso-asym-asym*-[Co<sub>2</sub>(tmpdne)(OH)<sub>2</sub>]<sup>4+</sup> showing 20% thermal displacement parameters.

**Table 2.** Selected Bond Lengths (Å) for *rac-asym-asym*-[Co<sub>2</sub>(tmpdne)(OH)<sub>2</sub>](ClO<sub>4</sub>)<sub>4</sub>·3H<sub>2</sub>O

Co(1)–O(01)	1.89(2)	Co(2)–O(02)	1.89(2)
Co(1)–N(1)	1.96(2)	Co(2)–N(6)	2.05(2)
Co(1)–N(2)	1.99(2)	Co(2)–N(7)	1.97(2)
Co(1)–N(3)	1.95(2)	Co(2)–N(8)	1.97(2)
Co(1)–N(4)	2.00(2)	Co(2)–N(9)	1.98(2)
Co(1)–N(5)	2.03(2)	Co(2)–N(10)	1.94(2)

to arise by deprotonation of one of the four inequivalent α-CH<sub>2</sub> protons. Although not directly proven for the present pair of complexes, it has been established<sup>9</sup> for the similar complex *asym*-[Co(dmptmetacn)Cl]<sup>2+</sup> which was the prototype (and likely also for the unsubstituted species *asym*-[Co(dmptacn)Cl]<sup>2+</sup>, although it has one NH<sup>10</sup>). Which particular proton that was involved was also established. However, deuteration experiments for the present set of dinuclear dichloro ions were inconclusive. Some exchange was observed at all four sites in OD<sup>-</sup>/DCl cycle experiments, as collapse of the α-CH<sub>2</sub> signals in the <sup>1</sup>H NMR and broadening of the α-CH<sub>2</sub> <sup>13</sup>C lines, consistent with reaction via methylene deprotonation but not proving it. Further, we could not determine which site was that effective in base hydrolysis since the product hydroxo ions also undergo CH exchange at the α-CH<sub>2</sub> centers.

In summary, the present series of complexes seem to provide further examples of the pseudoaminate mechanism, shown in Scheme 1. We have not established whether deprotonation is rate determining or a fast preequilibrium, either of which can account for the first rate dependence on [OH<sup>-</sup>], but the arguments presented elsewhere<sup>9,10</sup> indicate that all these species base hydrolyze by rate-limiting deprotonation. Also, the relative magnitude of the *k*<sub>OH</sub> values are consistent with a common pseudoaminate mechanism.

**Crystallography.** An ORTEP diagram of the *rac-asym-asym*-[Co<sub>2</sub>(tmpdne)(OH)<sub>2</sub>]<sup>4+</sup> cation is shown in Figure 9 along with the atomic numbering scheme. Selected interatomic parameters are listed in Tables 2 and 3. Additional crystallographic data are accessible from the deposited CIF file.

The molecule crystallizes in the achiral *P*2<sub>1</sub>/*a* space group. However each dinuclear ion is dissymmetric (ΛΛ or ΔΔ configurations) in principle but actually asymmetric because the two chiral mononuclear components are twisted about the ethylene bridge in the solid state, removing the 2-fold

**Table 3.** Selected Bond Angles (deg) for *rac-asym-asym*-[Co<sub>2</sub>(tmpdne)(OH)<sub>2</sub>](ClO<sub>4</sub>)<sub>4</sub>

O(01)–Co(1)–N(1)	96.7(9)	O(02)–Co(2)–N(6)	90.4(8)
O(01)–Co(1)–N(2)	174.6(9)	O(02)–Co(2)–N(7)	175.9(9)
O(01)–Co(1)–N(3)	88.7(9)	O(02)–Co(2)–N(8)	93.1(9)
O(01)–Co(1)–N(4)	93.1(8)	O(02)–Co(2)–N(9)	88.2(8)
O(01)–Co(1)–N(5)	90.2(8)	O(02)–Co(2)–N(10)	93.7(9)
N(1)–Co(1)–N(2)	82.6(9)	N(6)–Co(2)–N(7)	85.8(8)
N(1)–Co(1)–N(3)	94(1)	N(6)–Co(2)–N(8)	93.3(9)
N(1)–Co(1)–N(4)	170(1)	N(6)–Co(2)–N(9)	171(1)
N(1)–Co(1)–N(5)	94.4(9)	N(6)–Co(2)–N(10)	86(1)
N(2)–Co(1)–N(3)	97(1)	N(7)–Co(2)–N(8)	86(1)
N(2)–Co(1)–N(4)	87.9(8)	N(7)–Co(2)–N(9)	95.8(9)
N(2)–Co(1)–N(5)	84.5(9)	N(7)–Co(2)–N(10)	88(1)
N(3)–Co(1)–N(4)	85(1)	N(8)–Co(2)–N(9)	96(1)
N(3)–Co(1)–N(5)	172.0(9)	N(8)–Co(2)–N(10)	173(1)
N(4)–Co(1)–N(5)	87.5(8)	N(9)–Co(2)–N(10)	85(1)

rotational symmetry that is observed in solution (NMR). There are two cations of each enantiomer in the unit cell (*Z* = 4). The difference in structural parameters for the two halves of the dimer is evident (Tables 2 and 3).

The crystal structure clearly establishes the *rac* configuration for this dihydroxo ion derived with geometric retention from the faster eluting (Dowex) dichloro complex. However the relatively weak reflections severely diminished the accuracy compared to that for related structures, and only a few general comments can be made about the structural parameters (Tables 2 and 3). Both cobalt centers adopt the same *asym* stereochemistry as do all the dmptacn, dmpmetacn, daptacn, datn, and dats complexes thus far characterized.<sup>9,10,24–26</sup> The Co–N (amine and pyridine) bond lengths vary from 1.94(2) to 2.05(2) Å and tend to be longer than in [Co(dmptacn)OH<sub>2</sub>]<sup>3+</sup>, where they range from 1.906(7) to 1.937(7) Å. The ∠NCoN chelate ring angles for the tacn nitrogens in the complex are close to 90° (average 86.9°), and the same angles in the related complexes, [Co(dmptacn)OH<sub>2</sub>]<sup>3+</sup> and [Co(daptacn)Cl]<sup>2+</sup>, are on average 86.9 and 87.6°, respectively, very little different. The angles subtended by the pyridyl and tacn nitrogens (average 84.7°) are also less than 90° and again very similar to those found in the dmptacn and dmpmetacn derivatives. The Co–O(H) bond lengths (both 1.89(2) Å) in the dimer are, as expected, shorter than the corresponding Co–O(H)<sub>2</sub> distance<sup>26</sup> in the *asym*-[Co(dmptacn)OH<sub>2</sub>]<sup>3+</sup> species (1.945(6) Å).

**Acknowledgment.** W.G.J. and L.S. acknowledge financial support from the Australian Research Council. S.J.B. was the recipient of a Monash Graduate Scholarship.

**Supporting Information Available:** Table 1S, kinetic data, Figures 1S and 2S, <sup>13</sup>C NMR data, Figure 3S, a representation of complex ions, and a crystallographic file in CIF format for *rac-asym-asym*-[Co<sub>2</sub>(tmpdne)(OH)<sub>2</sub>](ClO<sub>4</sub>)<sub>4</sub>·3H<sub>2</sub>O. This material is available free of charge via the Internet at <http://pubs.acs.org>.

IC0400888

- (24) Fortier, D. G.; McAuley, A. J. *Chem. Soc., Dalton Trans.* **1991**, 101.  
 (25) Gahan, L. R.; Lawrance, G. A.; Sargeson, A. M. *Aust. J. Chem.* **1982**, *35*, 1119.  
 (26) McLachlan, G. A.; Brudenell, S. J.; Fallon, G. D.; Martin, R. L.; Spiccia, L.; Tiekink, E. R. T. *J. Chem. Soc., Dalton Trans.* **1995**, 439.